Insulin-dependent Interactions of Proteins with GLUT4 Revealed through Stable Isotope Labeling by Amino Acids in Cell Culture (SILAC)*

ARTICLE *in* JOURNAL OF PROTEOME RESEARCH · FEBRUARY 2006

Impact Factor: 4.25 · DOI: 10.1021/pr0502626 · Source: PubMed

9 AUTHORS, INCLUDING:

Leonard J Foster
University of British Columbia - Vancouver
180 PUBLICATIONS **7,308** CITATIONS
SEE PROFILE

Assaf Rudich
Ben-Gurion University of the Negev
120 PUBLICATIONS **6,778** CITATIONS
SEE PROFILE

Nish Patel
SickKids
15 PUBLICATIONS **822** CITATIONS
SEE PROFILE

Philip J Bilan
SickKids
72 PUBLICATIONS **3,041** CITATIONS
SEE PROFILE

research articles Journal of proteome research

Insulin-dependent Interactions of Proteins with GLUT4 Revealed through Stable Isotope Labeling by Amino Acids in Cell Culture (SILAC)*

Leonard J. Foster,[†,‡,#] Assaf Rudich,[§,#,⊥] Ilana Talior,[§,#] Nish Patel,[§] Xudong Huang,[§] L. Michelle Furtado,[§] Philip J. Bilan,[§] Matthias Mann,[†,||] and Amira Klip*[,§]

Center for Experimental BioInformatics (CEBI), Department of Biochemistry and Molecular Biology, University of Southern Denmark, Campusvej 55, DK-5230 Odense M, Denmark, UBC Centre for Proteomics and Department of Biochemistry and Molecular Biology, 301−2185 East Mall, University of British Columbia, Vancouver, BC, V6T 1Z4, Program in Cell Biology, Hospital for Sick Children, 555 University Ave., Toronto, ON, Canada M5G 1X8, and Department of Proteomics and Signal Transduction, Max-Planck Institute for Biochemistry, Martinsried, Germany D-82152

Received August 10, 2005

The insulin-regulated glucose transporter (GLUT4) translocates to the plasma membrane in response to insulin in order to facilitate the postprandial uptake of glucose into fat and muscle cells. While early insulin receptor signaling steps leading to this translocation are well defined, the integration of signaling and regulation of GLUT4 traffic remains elusive. Several lines of evidence suggest an important role for the actin cytoskeleton and for protein−protein interactions in regulating GLUT4 localization by insulin. Here, we applied stable isotope labeling by amino acids in cell culture (SILAC) to identify proteins that interact with GLUT4 in an insulin-regulated manner. Myc-tagged GLUT4 (GLUT4*myc*) stably expressed in L6 myotubes was immunoprecipitated via the *myc* epitope from total membranes isolated from basal and insulin-stimulated cells grown in medium containing normal isotopic abundance leucine or deuterated leucine, respectively. Proteins coprecipitating with GLUT4*myc* were analyzed by liquid chromatography/ tandem mass spectrometry. Of 603 proteins quantified, 36 displayed an insulin-dependent change of their interaction with GLUT4myc of more than 1.5-fold in either direction. Several cytoskeleton-related proteins were elevated in immunoprecipates from insulin-treated cells, whereas components of the ubiquitin-proteasome degradation system were generally reduced. Proteins participating in vesicle traffic also displayed insulin-regulated association. Of cytoskeleton-related proteins, α-actinin-4 recovery in GLUT4 immunoprecipitates rose in response to insulin 2.1 ± 0.5-fold by SILAC and 2.9 ± 0.8-fold by immunoblotting. Insulin caused GLUT4 and α-actinin-4 co-localization as revealed by confocal immunofluorescence microscopy. We conclude that insulin elicits changes in interactions between diverse proteins and GLUT4, and that cytoskeletal proteins, notably α-actinin-4, associate with the transporter, potentially to facilitate its routing to the plasma membrane.

Keywords: alpha-actinin 4 • L6 muscle cells • protein−protein interactions • mass spectrometry • quantitative proteomics • insulin • GLUT4 binding proteins

Introduction

The insulin-regulated glucose transporter GLUT4 is a member of the SLC2 family comprising GLUTs 1−12,[1] and is responsible for the majority of glucose uptake into skeletal muscle and fat cells.[2] Upon insulin stimulation, GLUT4 is recruited to the plasma membrane from intracellular vesicular pools, a process requiring dynamic changes in the actin cytoskeleton.[3−5] Insulin-induced stimulation of glucose uptake is critical for the maintenance of glucose homeostasis. Indeed, this process is impaired in insulin resistance, a hallmark of type 2 diabetes. In this disease, GLUT4 expression is attenuated in adipose tissue and type 1 oxidative muscle fibers,[6] sparking interest in processes regulating the half-life of the transporter. Since a protein's intracellular localization, traffic, activity, stability, and degradation may all be controlled through interactions with binding protein partners, identifying GLUT4-interacting proteins is of biological and clinical interest. Several potential GLUT4-binding partners have been proposed, mostly by pull-down experiments using GLUT4 C-terminal sequences

* To whom correspondence should be addressed. Tel.: (416) 813-6392. Fax: (416) 813-5028. E-mail: amira@sickkids.ca.
† University of Southern Denmark.
‡ University of British Columbia.
§ Hospital for Sick Children.
|| Max-Planck Institute for Biochemistry.
# These authors contributed equally to this work.
⊥ AR current address: S. Daniel Center for Health and Nutrition, Department of Clinical Biochemistry, Faculty of Health Sciences, Ben-Gurion University of the Negev, Beer-Sheva, 84103, Israel.

10.1021/pr0502626 CCC: $33.50
Published on Web 12/08/2005

fused to glutathione-s-transferase.[7−13] While providing important insights, these studies may be limited in their capacity to detect interactions with the complete protein sequence, which includes a large cytosolic loop as well as C- and N-terminal intracellular domains. Unfortunately, anti-GLUT4 antibodies are directed only against intracellular epitopes, which may be occupied by ligand proteins. Such a situation limits the use of anti-GLUT4 antibodies as a tool for a comprehensive analysis of the array of GLUT4-interacting proteins that are dynamically regulated by acute insulin stimulation.

Mass spectrometry-based proteomics has emerged as a powerful method for determining the composition of immunoprecipitated protein complexes.[14,15] Commercially available mass spectrometers and database search tools have advanced to the point where experienced laboratories can identify hundreds or thousands of proteins in exceedingly complex mixtures using nano-flow high performance liquid chromatography (HPLC)/ tandem mass spectrometry (LC−MS/MS).[16,17] The reliability of these protein identities is markedly augmented through the use of stringent acceptance criteria, such as enzyme specificity and high mass accuracy.[18] The classical approach of independent immunoprecipitations from different conditions can be confounded by the presence of nonspecifically interacting proteins and the nonquantitative nature of mass spectrometry restricts the ability to detect dynamic stimulus-induced alterations in the composition of a protein complex. Recently, we have applied stable isotope labeling by amino acids in cell culture (SILAC,[19]) to proteomic studies of protein complexes as a method for distinguishing functional (dynamic) protein−protein interactions from nonfunctional or nonspecific interactions with a solid-phase matrix or affinity bait.[20−22] Proteins that bind nonspecifically from labeled and unlabeled samples will bind equally well to the bait, presenting a ratio near 1.0, whereas proteins whose binding depends on the functional condition of the experiment will yield a ratio of greater than or less than 1.0. Independently, Ranish et al. developed a similar approach[23] using isotope coded affinity tags.[24] The incorporation of the quantitative dimension provided by SILAC or isotope tags is critical as, in our experience, the fraction of nonspecific or nonfunctional interactions present in an isolated complex can be as high as 99% and can easily mask biologically relevant interactions of low affinity.[20−22]

Here, we apply SILAC to identify proteins interacting with GLUT4 in an insulin-dependent manner using a skeletal muscle cell line that stably expresses GLUT4 tagged with a *myc* epitope in its first exofacial loop (GLUT4*myc*). Immunoprecipitation via antibodies that recognize the noncytosolic tag on GLUT4*myc* allows for the identification of proteins that could associate with the transporter throughout its cytosol-facing sequences.

Experimental Procedures

Materials. Sequencing grade modified porcine trypsin was purchased from Promega (Mannheim, Germany). Endopeptidase LysC was obtained from Wako (Osaka, Japan). Chromatography solvents were purchased from Sigma-Aldrich Denmark A/S (Copenhagen, Denmark). L-leucine-5,5,5-D_3 was purchased from Cambridge Isotope Laboratories, Andover, MA). Normal isotopic abundance leucine and Protease Inhibitor Cocktail were from Sigma (St. Louis, MO). Fetal bovine serum, α-MEM standard culture medium and other tissue culture reagents were purchased from Wisent Inc. (Toronto, ON). Leucine-deficient α-MEM media was purchased from JRH Biosciences Inc., (Lenexa, Kansas, USA). *N*-hydroxysuccinimide-activated Sepharose 4 FastFlow beads and Sepharose CL-6B beads were from Amersham Biosciences/ Pharmacia (Piscataway, NJ). Rabbit polyclonal antibodies for α-actinin-4, was from Alexis Biochemicals (San Diego, CA). Antibody to GAPDH (sc-25778) and Monoclonal (9E10) anti-*myc* were purchased from Santa Cruz Biotechnology (Santa Cruz, CA). Horseradish peroxidase-conjugated secondary antibodies were obtained from Jackson ImmunoResearch (West Grove, PA).

Stable Isotope Labeling of Cultured L6 Myoblasts. L6-GLUT4*myc* myoblasts were grown and differentiated into myotubes as described[25] but with the following modifications: Cells were seeded on 10 cm dishes and grown in leucine-deficient α-MEM (JRH Biosciences Inc., Lenexa, Kansas, USA) supplemented with 2% (v/v) fetal bovine serum (FBS) that was dialyzed against PBS for 4 h at 4 °C to deplete it of amino acids (10 000 molecular weight cutoff), 1% (v/v) ampicillin-streptomycin antibiotic solution, and 52.4 mg/L of either normal isotopic abundance leucine (LeuD0, Sigma) or leucine with three deuterium atoms (L-Leucine-5,5,5-D3, LeuD3). Seven days after seeding, myotubes were serum-starved for 3 h in the same medium devoid of FBS, and then stimulated for 10 min without or with 100 nM insulin, respectively. To eliminate the possibility of isotopic effects, we switched the LeuD0 and LeuD3 labels between the basal and insulin-stimulated conditions several times and this did not impact the insulin effect observed on GLUT4-interacting proteins. In addition, the 7 days incubation of L6-GLUT4*myc* cells with LeuD3 had no effect on the cultures compared to cells cultured with LeuD0. In preliminary experiments we found that immunoprecipitating GLUT4myc directly from whole cell lysates resulted in excessive levels of myosin in the immune complexes that masked many less abundant proteins. We found that by initially isolating total membranes (TM) from LeuD0- and LeuD3-labeled myotubes cultures the levels of highly abundant muscle cytoskeletal proteins were markedly reduced. To prepare TM, myotubes (10 or 30 × 10 cm dishes per condition for regular or large-scale experiments, respectively) were washed with ice-cold PBS and then with homogenization buffer (250 mM sucrose, 20 mM HEPES, pH 7.4, 1 mM EDTA, 1 mM sodium vanadate, 10 nM okadaic acid and 1:1000 dilution of Protease Inhibitor Cocktail). Cells were then scraped in the same buffer, and homogenized by 12 strokes in a Teflon-glass Wheaton homogenizer, followed by centrifugation (700 × *g* for 10 min at 4 °C). The supernatants were collected and pellets were re-suspended and homogenized twice more as described above. To obtain TM, supernatants were centrifuged (195 000 × *g* for 75 min at 4 °C) and pellets were collected in 1.5 mL PBS containing 0.2% (v/v) $C_{12}E_8$, phosphatase and protease inhibitors as above, homogenized, and rotated for 15−30 min at 4 °C to allow solubilization by the detergent (∼3 mg protein/mL). Thereafter, TM were centrifuged in a tabletop microfuge (14 000 × *g* for 15 min at 4 °C), the supernatant was collected and protein content determined (bicinchoninic acid method). This final centrifugation removed large cytoskeletal structures prior to immunoprecipitation of GLUT4*myc*.

Immunoprecipitation of GLUT4myc. Mouse monoclonal 9E10 IgG anti-*myc* antibody (200 μg) were first passed through protein G columns (Pierce Biotechnology Inc., Rockford, IL), eluted, and dialyzed against PBS prior to being covalently linked to *N*-hydroxysuccinimide-activated Sepharose 4 FastFlow beads (1 mL wet volume) according to the manufacturer's instructions. The Sepharose beads conjugated to anti-*myc* were

suspended in PBS pH 7.4 (50% v/v; 100 μg antibody/ml bead suspension).

Equal amounts of TM protein from LeuD3-labeled, insulin-stimulated cells, and unlabeled nonstimulated (basal) cells were mixed for the immunoprecipitation of GLUT4 (0.55 and 5.0 mg protein of each for regular and large-scale experiments, respectively). The mixed TM samples were first pre-cleared with Sepharose CL-6B beads (0.05 or 0.5 mL of 50% v/v suspension, as required) with rotation for 30 min at 4 °C, then immunoprecipitation was carried out overnight at 4 °C with Sepharose beads containing anti-*myc* antibody (0.04 or 0.4 mL of 50% v/v suspension, as required). Thereafter, beads were precipitated by slow (30 s, 950 × *g*) spins, washed twice with PBS containing inhibitors and 0.2% $C_{12}E_8$, and once with PBS before addition of 150 μL of modified SDS-PAGE sample buffer (5% (w/v) SDS, 25% (v/v) glycerol, and 156 mM Tris-HCl pH 6.8, without β-mercaptoethanol and bromophenol blue) and incubation for 15 min at 65 °C.

LC−MS/MS, Database Searching and Quantification. In initial experiments, the immune complex was extracted in 200 μL 6 M urea/2 M thiourea (in 20 mM Tris, pH 8.0) and prepared for LC−MS as described.[26] In later experiments, the immune complexes were solubilized in modified SDS-PAGE sample buffer and subjected to one-dimensional gel electrophoresis. Proteins were then visualized with colloidal Coomassie blue, each lane cut into 10 slices and then subjected to in-gel digestion.[27] Peptide digests were desalted using STAGE tips[28] and loaded onto reversed phase analytical columns for liquid chromatography.[29] Peptides were eluted from the analytical columns by 100 min gradients comprised of three linear steps running from 5.6% to 64% acetonitrile and sprayed directly into the orifice of a linear ion-trap-Fourier transform mass spectrometer (Finnigan LTQ-FT, Thermo Electron). The LTQ-FT was set to acquire tandem mass spectra of the five most abundant multiply charged peptides per ~2 s cycle. Survey scans were acquired at 100 000 resolution using the FT detector while fragment spectra were simultaneously acquired on the linear ion-trap detector. All fragment spectra were then searched, using Mascot Server (Matrix Science), against the most recent rat IPI protein database (v1.19, 33 572 entries) that had been supplemented with sequences for human keratins, mouse immunoglobulins, bovine serum albumin, porcine trypsin and endopeptidase LysC. The following search criteria were used in all cases: tryptic cleavage with a maximum of one missed cleavage, ion-trap fragmentation characteristics, 10 parts per million (ppm) error tolerance for precursor ion masses (measured in FT), 0.5 Da error tolerance for product ion masses (measured in LTQ), methionine oxidation and leucine with three deuterium atoms as variable modifications and cysteine carbamidomethylation as a fixed modification. Fragment spectra were extracted from Xcalibur RAW files and charge states assign using the Extract_MSN script (Thermo Electron), requiring a minimum ion intensity of 10 for each peak and a minimum of 5 peaks per spectrum. Charge states and monoisotopic peak assignments were then double-checked using DTA-SuperCharge, an in-house script, before DTA files were combined into a single Mascot Generic Format file.

Acceptance criteria for peptide and protein identifications were determined by searching 5400 random fragment spectra against forward and reversed rat IPI databases (see ref 17 for an introduction). After removing redundant peptide sequences, 929 unique peptide sequences with scores greater than 24, more than 7 amino acids in length and with mass accuracies better than 10 ppm were identified in the normal database, while only 8 similar sequences were identified in the reversed database. These results indicate a false positive identification rate of 8/929, or 0.9%, at the peptide level. Therefore, proteins were only considered *identified* if at least two unique peptides of this quality were sequenced among all experiments, giving a statistical confidence of more than 99.99% at the protein level, or less than one false positive protein identification in ten thousand. Application of these criteria to the entire data set led to the identification of 970 unique protein sequences. Multiple isoforms of a protein were only kept in the final list if they were differentiated by at least one unique peptide meeting the above criteria; however, each isoform was still required to have at least two peptides identifying it. Insulin:control ratios were calculated based on the integration of extracted ion chromatograms generated from survey scans using MSQuant[22] (http://msquant.sourceforge.net), after accounting for the reversed phase shift due to deuterated leucine. The average measured ratio of GLUT4*myc* was initially 0.91 so this was adjusted to 1.0 and all other ratios were corrected accordingly. Since quantification was based on leucine, peptides that did not contain any leucine residues were not quantifiable. Additionally, where the peptide ion signal was too close to the noise level no reliable quantification was possible. Nonetheless, of the 970 identified proteins we were able to quantify 603. All peptide and protein information was stored in an in-house relational database for subsequent querying.

Gene Ontology Classification. UniProt accession numbers of all 603 quantified proteins and the subset of 36 proteins displaying a ratio greater than 1.5 or less than 0.66 based on at least three peptides were classified using the GOMiner tool (http://discover.nci.nih.gov/gominer/) as described.[30] Distributions of these two sets of proteins within the subcategories of the Cellular Physiological Process category (GO:0050875) were then graphed.

Detection of α-Actinin-4 and GAPDH in GLUT4myc Immunoprecipitates by Immunoblotting. L6 myoblasts seeded in four 10-cm dishes and grown to confluence or differentiated into myotubes were deprived of serum for 4.5 h at 37 °C, and then treated without or with 100 nM insulin for 20 min at 37 °C. The cells were washed with cold PBS, scraped with lysis buffer (150 mM NaCl, 2 mM EDTA, 1% (vol/vol) Triton X-100, 20 mM iodoacetamide, 50 mM *N*-octylglucoside and Protease Inhibitor Cocktail, 20 mM Tris-HCl, pH 8.0), passed through 27.5 gauge syringe and incubated on ice for 2 h. The lysates were centrifuged (13 000 × *g*) for 15 min at 4 °C and supernatants were quantified for protein concentration using the bicinchoninic acid method. Equal amounts of protein (1.5 mg of protein/reaction) from each sample were immunoprecipitated with 40 μL of myc antibody conjugated to Sepharose beads with rotation overnight at 4 °C. Beads were collected by centrifugation for 30 s at 950 × *g* at 4 °C and washed 5× with wash buffer (150 mM NaCl, 2 mM EDTA, 1% (vol/vol) Triton X-100, 20 mM iodoacetamide, Protease Inhibitor Cocktail, 20 mM Tris-HCl, pH 8.0) by gentle rotation for 10 min at 4 °C. Beads were then resuspended in 20 μL of lysis buffer plus 20 μL SDS-PAGE sample buffer (2% (w/v) SDS, 5% (v/v) β-mercaptoethanol, 10% (v/v) glycerol, 0.005% (w/v) bromophenol blue and 62.5 mM Tris-HCl pH 6.8) and heated at 100 °C for 3 min. Proteins were separated by 5 or 10% polyacrylamide (vol/vol) SDS-PAGE, transferred onto PVDF membranes and blotted with anti-α-actinin-4 (1:2000), anti-GAPDH (1:1000) or anti-*myc* (1:500) antibodies. Immunoreactive bands were visualized

with Horseradish peroxidase-conjugated secondary antibodies and enhanced chemiluminescence.

Fluorescence Microscopy. L6-GLUT4*myc* myotubes grown on 25 mm diameter glass coverslips were deprived of serum for 4 h, and then treated with 100 nM insulin for 5 min at 37 °C. Labeling of actin filaments with rhodamine-coupled phalloidin and immunostaining of specific antigens was carried out as described previously.[31] It was essential to fix the cells at 4 °C immediately after insulin stimulation and to permeabilize in 0.1% (vol/vol) Triton X-100 for 3 min in order to preserve actin morphology. The primary antibody dilution factors were as follows: *myc* monoclonal, 1:150 or α-actinin-4 polyclonal, 1:250 in 0.1% (wt/vol) BSA/PBS. To label actin filaments simultaneously with any of the above listed molecules, fixed and permeabilized cells were incubated for 1 h at room temperature with the fluorophore-conjugated phalloidin indicated in the figure legends (0.01 U/ coverslip) during the incubation with the secondary antibody. To eliminate artifactual "co-localization" in these co-staining experiments, fluorophores with maximal spectral separation were chosen. The staining pattern observed in co-staining experiments was compared to that with single-staining experiments using the same antibody. Cells were examined with a Zeiss LSM 510 laser scanning confocal microscope using multichannel scanning to reduce the possibility of cross-talk between fluorophores. Acquisition parameters were adjusted to exclude saturation of the signal.

Results

SILAC Approach to Immunoprecipitations. Affinity-based methods are often used to isolate proteins interacting with a target of interest and powerful, mass spectrometry-based proteomics tools[32] employed to analyze the resulting complexes. However, biologically interesting protein−protein interactions may be weak or transient, so excessive washing of isolated complexes can interfere with their detection. Alternatively, light washing can preserve such interactions but highly abundant or generally 'sticky' proteins that bind nonspecifically to the affinity matrix present a high background that can easily mask specific interactions. We used SILAC to overcome some of these issues, and the principle of this approach is depicted in Figure 1. GLUT4*myc* was immunoprecipitated from insulin-stimulated cells whose proteome had been SILAC-labeled with LeuD3 (L-Leucine-5,5,5-D3), and from nonstimulated cells whose proteome had been labeled with LeuD0 (normal isotopic abundance leucine). Eluates were mixed and two versions of each Leu-containing peptide were detected. By calculating the ratio between the MS peak derived from a peptide with LeuD3 (in this case, from insulin-stimulated cells) and the peak from the respective LeuD0 (basal), a ratio value of 1.0 would indicate no change in the abundance of this protein in the basal compared to the insulin-stimulated state within the GLUT4*myc* immunoprecipitate, whereas a value higher or lower than one would indicate that insulin increased or decreased, respectively, the abundance of the specific peptide.

Protein Identification and Quantification. Isolated GLUT4*myc* immune complexes were analyzed by one-dimensional gel electrophoresis followed by liquid chromatography/mass spectrometry, as described in Experimental Procedures. Figure 2a shows the total ion chromatogram from a typical analysis of one gel slice. Survey scans (Figure 2b) at 100 000 resolution were measured approximately every 2 s throughout the LC gradient and peptide ions detected (such as TFDQI-

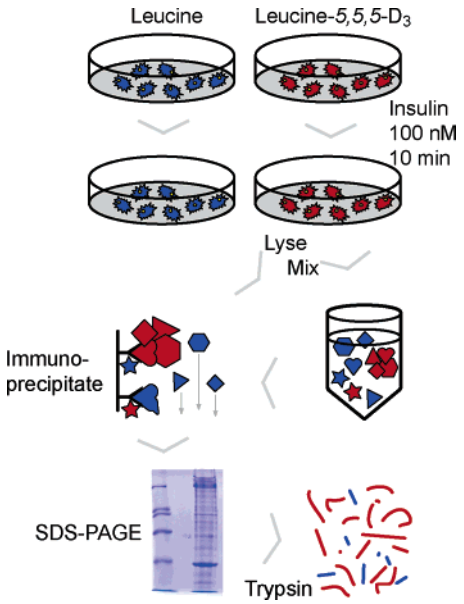

Figure 1. Application of SILAC to identify specific, insulin-dependent binding partners from background binders. Two populations of GLUT4*myc* -expressing L6 myotubes are cultured in media containing either leucine with three hydrogen atoms replaced by deuterium (L-leucine-*5,5,5*-D_3; LeuD3) or normal isotopic abundance leucine (LeuD0). One population (the LeuD3 population in this study) is stimulated for 10 min with 100 nM insulin before both populations are processed for total membranes, solubilized, combined and subjected to immunoprecipitation with 9E10 anti-*myc* antibody as detailed in Experimental Procedures. Isolated immune complexes are eluted, resolved by one-dimensional SDS-PAGE and digested to peptides for analysis by LC/MS. Peptides from proteins whose interactions with GLUT4*myc* are insulin-dependent will show higher or lower abundance in the LeuD3 form (red) if insulin enhances or reduces, respectively, their interactions with GLUT4*myc*. Peptides from proteins whose binding are not affected by insulin or are bound nonspecifically (blue) will be present at equal proportions of LeuD0 and LeuD3 labeling in the GLUT4*myc* immunoprecipitates.

SATFR from GLUT4 depicted in Figure 2c), were fragmented in the LTQ. After discounting modifications and charge states, 9754 unique peptides were sequenced and their masses measured to an average accuracy of 2.39 ppm. Nine-hundred seventy proteins, their sequences covered to an average of 24%, were identified from these peptides (Supporting Information Table 1) with an estimated false:positive ratio < 1:10 000 (see Experimental Procedures).

Sequenced peptides were quantified on the basis of their extracted ion chromatograms (Figure 2d) and insulin:control ratios for each protein were calculated as the average ratios observed in all experiments for 603 proteins (Supporting Table 1). While the ratios ranged from 0.3 to 4.0 (Figure 2e), the presence of most proteins in the immune complex was not affected by insulin, consistent with previous estimations of the prevalence of 'bona fide' interactions in a protein complex.[20−22] The average relative standard error of the mean for the in insulin:control ratios was 26%, similar to previous reports using SILAC (LeuD3: LeuD0 ratios) with other types of stimuli.[26,33] Thirty-six proteins (Tables 1A and 1B) with insulin:control ratios greater than 1.5 or lower than 0.66 (1/1.5) for at least three peptides were identified. A cutoff value of 1.5 was selected as this was approximately twice the standard error of the popula-

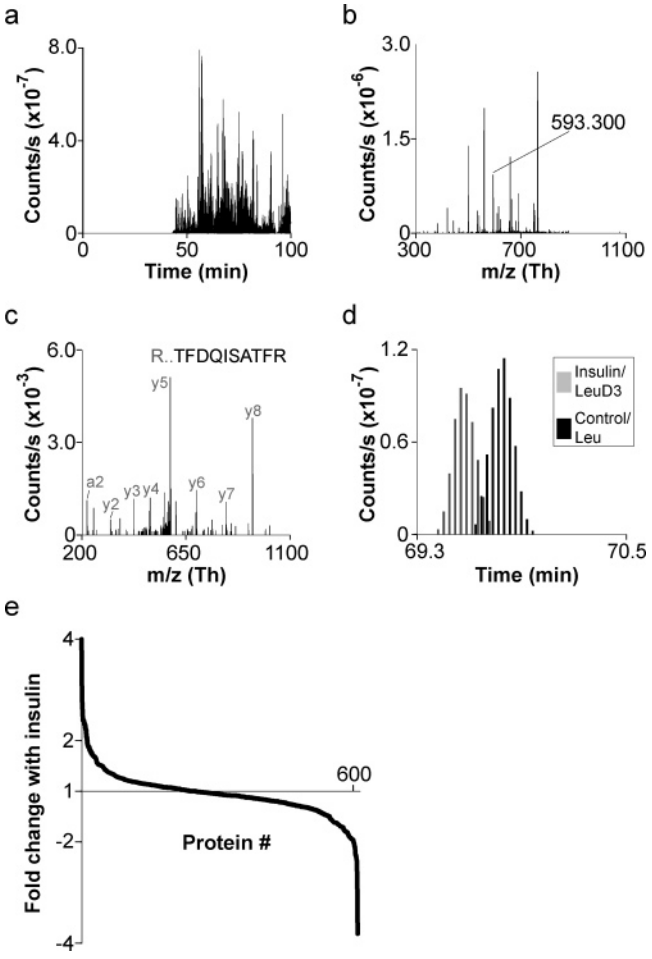

Figure 2. Application of SILAC to determine specific binding partners. **(a)** Peptide mixtures from in-gel digested proteins were resolved by reversed phase HPLC (see Experimental Procedures) and sprayed directly into the orifice of an LTQ-FT. **(b)** Survey scans of peptides eluted from reversed phase columns were acquired and used to select peptide ions for fragmentation. Fragment spectra **(c)** of the 593.3 ion from **(b)** was found to match the TFDQISATFR peptide from GLUT4. **(d)** Representative extracted ion chromatogram for the LISEEDLLK peptide from GLUT4*myc* demonstrating an insulin:control (LeuD3/LeuD0) ratio of 0.91. **(e)**, Plot of insulin:control ratios for all proteins quantified in this study, ranked from largest to smallest.

tion and was deemed to represent the minimum biologically significant change.[20,21,33] Moreover, the insulin-dependent changes in surface GLUT4 levels are in the range 1.5 to 2.2-fold in muscle cells. As an additional measure of confidence, we only considered those proteins where a standard deviation could be calculated (i.e., based on at least three peptides).

Proteins Exhibiting Dynamic, Insulin-Regulated Association with GLUT4 as Identified by SILAC. Some general trends were observed for the entire cohort of 603 proteins. For example, several ubiquitin-proteasome components or other proteases showed reduced interaction with GLUT4 in the insulin-treated samples (ratio < 1), whereas those involved in protein synthesis and protein folding tended to display enhanced association with GLUT4 (ratio > 1) (Supporting Information Table 1). Proteins with insulin:control ratio > 1.3 and <1.5 (Supporting Information Table 1) may also be of future interest. Among these, some metabolic enzymes associated with GLUT4*myc* immunoprecipitates in an insulin-regulated manner including aldolase A (previously reported as a GLUT4-interacting protein[11]). Proteins identified in Table 1 showed the highest dynamic changes (greater than 1.5-fold) in their interaction with GLUT4 in response to insulin. Of these 36 proteins, several cytoskeleton-associated proteins such as α-actinins 1 and 4 and cofilin displayed an insulin:control ratio > 1.5, suggesting that insulin augmented their association with GLUT4. Similarly, proteins involved in intracellular traffic, had either insulin:control ratios >1.5 and increased association with GLUT4 in response to insulin (Arfs 3 and 5) or insulin:control ratios <0.66 and decreased association with GLUT4 in response to insulin (Rab7 and NSF). Of note, association of the glycolytic pathway enzyme GAPDH with GLUT4 was also enhanced upon insulin treatment (insulin:control ratio of 1.6).

The sheer volume of information returned from a proteomic analysis can make it difficult to discern biological meaning in the data. One commonly used approach to further distill proteomic data is to classify the proteins according to their functional categories using the Gene Ontology system.[34] To this end, we have classified all proteins for which ratios were measured (total of 603) and the subset of those proteins for which reliable ratios (i.e., based on three or more peptides) changing more than 1.5-fold were observed (total of 36). The distribution of these proteins in the subcategories within Cellular Physiological Processes is depicted in Figure 3. The 603 proteins distributed across a wide range of categories as would be expected for nonspecifically binding proteins. Consistent with the ability of SILAC to differentiate dynamic binding partners from static or nonspecific ones, the proteins that displayed insulin-dependent binding to GLUT4 were enriched in categories associated with intracellular movement of proteins (e.g., Protein Transport−GO:0015013) or specific metabolic pathways (e.g., Generation of Precursor Metabolites and Energy−GO:0006091, Monosaccharide Metabolism − GO:0005996), two of the main functions that insulin regulates.

Substantiation of the Binding of GAPDH, a Glycolytic Protein, to GLUT4. A functional analysis of the role of GLUT4-binding proteins in GLUT4 cycling, stability or activity is clearly beyond the scope of this study. Similarly, a comprehensive verification by immunoblotting or immunocytochemistry of the insulin-dependent association of all other proteins listed in Table 1 is a substantive task that will soon be undertaken, step-by-step. However, we found it compelling to verify the effect of insulin on the binding to GLUT4 of Glyceraldehyde 3-phosphate dehydrogenase (GAPDH), a metabolically relevant protein. GAPDH is an enzyme in the glycolytic pathway that, coupled to 3-phosphoglycerate kinase, generates ATP in the absence of oxidative metabolism. This enzyme is particularly interesting because, in addition to its role in glycolysis, it associates with synaptic vesicles where production of ATP fuels neurotransmitter reuptake.[35] Importantly, the results in Table 1 show that insulin stimulation of L6 myotubes led to a 1.6 ± 0.1-fold increase in binding of GAPDH to GLUT4*myc*. These results are further confirmed in Figure 4, by immunoblotting of GLUT4*myc* immunoprecipitates with anti-GAPDH antibody. These observations lay the foundation for future analysis of the potential interplay between GAPDH and GLUT4 in diverse cellular functions.

α-Actinin-4 as a Model Protein with Insulin-Dependent Binding to GLUT4. Among the cytoskeletal proteins listed in Table 1, α-actinin-4 showed a prominent increase in binding to GLUT4 in response to insulin (insulin:control ratio 2.1 ± 0.5, Table 1). To confirm the quantitative aspect of SILAC in this

Table 1. Insulin-Dependent GLUT4*myc*-Associating Proteins[a]

accession	description	ins/con ± SEM	coverage (%)
	A. Proteins Whose Association with GLUT4*myc Increased* by Insulin		
	Cytoskeleton-Related		
Q9Z1P2	α-actinin-1	1.5 ± 0.2	56
P45592	Cofilin	1.7 ± 0.3	65
O43707	α-actinin-4	2.1 ± 0.5	44
	Vesicular and Traffic-Related		
P26473	ADP-ribosylation factor 5	1.5 ± 0.2	56
P26437	ADP-ribosylation factor 3	1.5 ± 0.2	59
Q7TNP1	Basigin 2	1.7 ± 0.6	14
	Metabolic and Signaling Enzymes		
Q6P6R2	Dihydrolipoamide dehydrogenase	1.5 ± 0.2	36
P04797	GAPDH	1.6 ± 0.1	59
	Protein Synthesis and Folding		
Q63081	Protein disulfide isomerase A6	1.5 ± 0.1	59
P29457	47 kDa heat shock protein	1.6 ± 0.1	54
Q9R1J8	Leprecan	2.4 ± 0.4	32
O88638	Putative eps protein	1.7 ± 0.5	31
Q64375	Synaptonemal complex protein SC65	1.9 ± 0.2	18
XP_340902	65kDa FK506-binding protein	1.9 ± 0.4	21
XP_237828	SDF2 like protein 1	2.6 ± 0.5	58
	B. Proteins Whose Association with GLUT4*myc Decreased* by Insulin		
	Cytoskeleton-Related		
Q9ER30	Sarcosin	0.6 ± 0.2	11
	Vesicular Traffic-Related		
P09527	Rab-7	0.6 ± 0.1	42
O88960	*N*-ethylmaleimide sensitive factor	0.6 ± 0.2	16
	Metabolic and Signaling Enzymes		
P09456	PKA I regulatory subunit	0.29 ± 0.02	11
P27881	Hexokinase type II	0.42 ± 0.02	4
P07872	Acyl-coenzyme A oxidase 1	0.6 ± 0.1	39
XP_341876	Isocitrate dehydrogenase	0.7 ± 0.2	47
	Proteasome-Ubiquitin and Protein Degradation-Related Proteins		
Q9EQX9	Ubiquitin-conjugating enzyme E2N	0.5 ± 0.2	40
Q63446	Polyubiquitin	0.6 ± 0.1	15
P24268	Cathepsin D	0.6 ± 0.1	30
XP_226439	26S proteasome regulatory subunit 7	0.64 ± 0.05	34
	Protein Synthesis and Folding		
Q91XW0	Heat shock protein 86	0.5 ± 0.1	20
	Miscellaneous		
XP_234709	KIAA1228	0.4 ± 0.1	8
XP_236180	Similar to complement-c1q TNF-related	0.46 ± 0.04	15
P58405	Striatin 3	0.51 ± 0.04	8
Q62667	Major vault protein	0.6 ± 0.1	37
XP_215022	FLJ22728	0.6 ± 0.1	18
XP_228865	FLJ10613	0.6 ± 0.1	5
Q9JHU5	Arfaptin 1	0.6 ± 0.1	27
XP_214321	RIKEN 6430517J16	0.61 ± 0.03	10

[a] Listed are proteins identified in this study whose insulin-dependent association with GLUT4 increased or decreased by more than 1.5-fold (1/1.5 = 0.66). UniProt or RefSeq accession numbers are listed, along with the protein name, the insulin:control ratio ± the standard error of the mean (SEM). The sequence coverage for each protein is also listed.

study, we chose α-actinin-4 for further biochemical and immunocytochemical characterization vis a vis GLUT4. By six independent immunoblot experiments, insulin increased the co-immunoprecipitation of α-actinin-4 with GLUT4*myc* in both myoblasts and myotubes (Figure 5a). The average fold increase in the association was 2.9 ± 0.8-fold, as determined by scanning densitometry of X-ray films exposed in the linear range of the chemiluminescence signal and quantification with NIH Image J software. As a negative control, wild-type L6 myotubes not expressing GLUT4*myc* subjected to immunoprecipitation using anti-*myc* antibody did not yield α-actinin-4 upon immunoblotting (Figure 5a). The immunoprecipitated samples were also immunoblotted for GLUT4*myc* protein levels, demonstrating equal loading of the GLUT4*myc* samples, to which the α-actinin-4 changes were adjusted (Figure 5a).

To understand if the association of α-actinin-4 with GLUT4*myc* was dependent on the integrity of the actin cytoskeleton, in three experiments L6-GLUT4myc myotubes were pretreated with 250 nM latrunculin B for 20 min prior to addition of insulin (or vehicle) in the continued presence of latrunculin B. This treatment prevents the insulin-stimulated rearrangement of F-actin in L6 myotubes[36] and, as shown in Figure 5b, it reduced the basal and insulin-stimulated association of α-actinin-4 with GLUT4*myc*. This result suggests that the association between GLUT4 and α-actinin-4 mostly occurs in the context of a dynamic actin cytoskeleton. Again as a negative control, wild-type L6 myotubes not expressing GLUT4*myc* subjected to immunoprecipitation using anti-*myc* antibody did not yield α-actinin-4 upon immunoblotting (Figure 5b). The immunoprecipitated samples were also immunoblotted for GLUT4*myc*

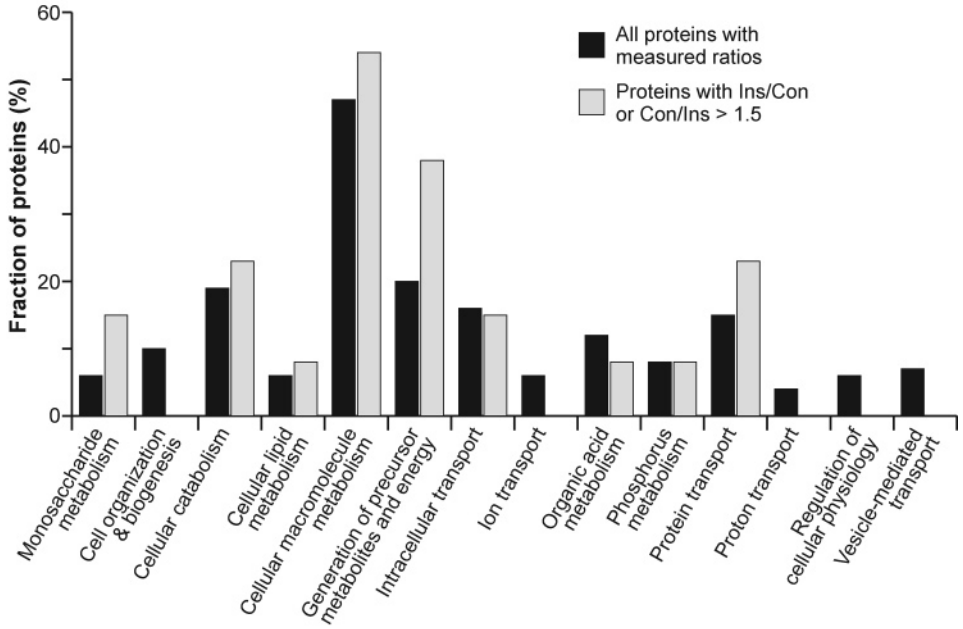

Figure 3. Functional ontologies of GLUT4*myc*-binding proteins. All 603 proteins (black bars) whose insulin-dependent interactions with GLUT4*myc* were measured in this study and the subset of 36 proteins (gray bars) whose binding changed more than 1.5-fold were classified according to their Gene Ontology (GO) annotation using GOMiner (see Experimental Procedures). The numbers of proteins assigned to each functional category are represented as fraction of the total number of proteins for which ontological information was available (ontological information was available for 318 of 603 proteins overall and for 23 of 36 insulin-affected proteins). Those categories with five or fewer proteins in the "All" category (black bars) are not shown for clarity. Numbers for each group do not necessarily add up to 100% because some proteins could be assigned to more than one category.

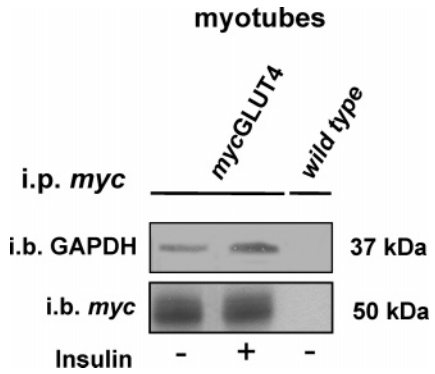

Figure 4. Insulin-dependent association of GLUT4*myc* with GAPDH detected by immunoblotting. L6-GLUT4*myc* or wild type myotube cultures were serum-deprived for 4.5 h and subsequently treated with or without 100 nM insulin for 20 min at 37 °C as indicated (±). Cells were lysed as described in Experimental Procedures and 1.5 mg of protein was immunoprecipitated with anti-*myc* antibody (9E10)-conjugated beads (i.p. *myc*). Following immunoprecipitation the beads were collected, washed, resuspended and subjected to SDS-PAGE in preparation for immunoblotting (i.b.) with anti-GAPDH (top gel; ~37 kDa) or anti−*myc* (bottom gel; ~50 kDa) antibodies. Immunoprecipitates from L6-GLUT4*myc* or L6 wild-type cells were loaded as indicated. Wild-type cells provide a negative control illustrating the specificity of binding of GAPDH to immunoprecipitated GLUT4*myc* in the first two lanes. Shown is a representative result of 2 experiments.

protein levels and represent a loading control for all immunoblots to which the α-actinin-4 changes were adjusted (Figure 5b).

To explore the spatial relationship between GLUT4, α-actinin-4 and actin in intact cells, we analyzed the localization of these proteins in L6 myotubes by laser confocal immunofluorescence microscopy. In unstimulated (basal state) myotubes, the majority of GLUT4*myc* was located in perinuclear regions of the myotubes (approximately 2 μm above the coverslip) and showed no colocalization with α-actinin-4 (Figure 6a, Merge). It is noteworthy that the confocal plane shown in Figure 6a cuts along the middle of the myotube in order to focus on the major GLUT*myc* depots and there were few noticeable actin stress fibers in this region. Insulin acutely promotes dorsal actin remodeling causing membrane ruffles in these cells,[37,38] and therefore the fluorescent images of α-actinin-4, GLUT4*myc* and actin shown in Figure 6b focus on the dorsal plane of the myotubes (approximately 4 μm above the coverslip). The 'Merge' image illustrates marked colocalization between these three proteins at the dorsal surface of myotubes. This 'Merge' image has been subjected to deconvolution to minimize contribution of fluorescent signal from adjacent planes. The areas of coincidence between α-actinin-4, GLUT4*myc* and actin within the outlined area (Figure 6b, inset a) were further analyzed by imaging Volocity 3.0® software (Improvision Inc. MA). The areas of coincidence for all three proteins thus defined are shown as white overlays in Figure 6b, inset b. It is clear that all three proteins partly colocalize at this improved level of resolution.

Discussion

The objective of this study was to identify proteins that bind to full-length GLUT4 in an insulin-dependent fashion. Previous studies searching for GLUT4 partners had, for the most part, focused on binding to selective segments of GLUT4 and usually in basal conditions. Thus, two-hybrid screens performed by several groups with cDNA libraries from human cardiac muscle, skeletal muscle or mouse TA1 adipocytes, used the C-terminal domain of GLUT4 as bait, and identified the C109 myosin-

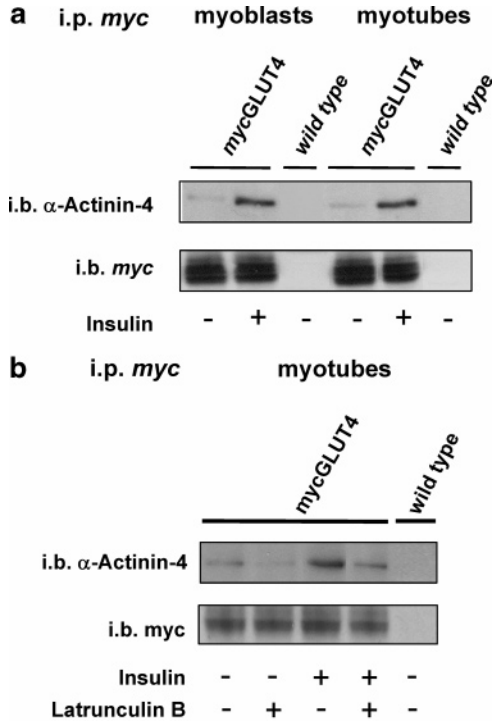

Figure 5. Insulin-dependent association of GLUT4*myc* with α-actinin-4 detected by immunoblotting and the effect of latrunculin B pretreatment. **(a)** L6-GLUT4*myc* or wild type myoblast or myotube cultures were serum-deprived for 4.5 h and subsequently treated with or without 100 nM insulin for 20 min at 37 °C as indicated (±). Cells were lysed as described in Experimental Procedures and 1.5 mg of protein was immunoprecipitated with anti-*myc* antibody (9E10)-conjugated beads (i.p. *myc*). Following immunoprecipitation the beads were collected, washed, resuspended and subjected to SDS-PAGE in preparation for immunoblotting (i.b.) with anti-α-actinin-4 (top gel; ∼100 kDa) or anti−*myc* antibodies (bottom gel; ∼50 kDa). Immunoprecipitates from L6-GLUT4*myc* or L6 wild-type cells were loaded as indicated. Shown is a representative result of 4 to 6 experiments. **(b)** L6-GLUT4*myc* or wild type myotube cultures were serum-deprived for 4.5 h and subsequently treated with or without 250 nM latrunculin B for 20 min at 37 °C as indicated (±), followed by treatment with 100 nM insulin for 20 min at 37 °C as indicated (±) in the continued presence or absence of latrunculin B. Cells were then processed for immunoprecipitation and immunoblotting as described in **(a)**. Shown is a representative result of 3 experiments.

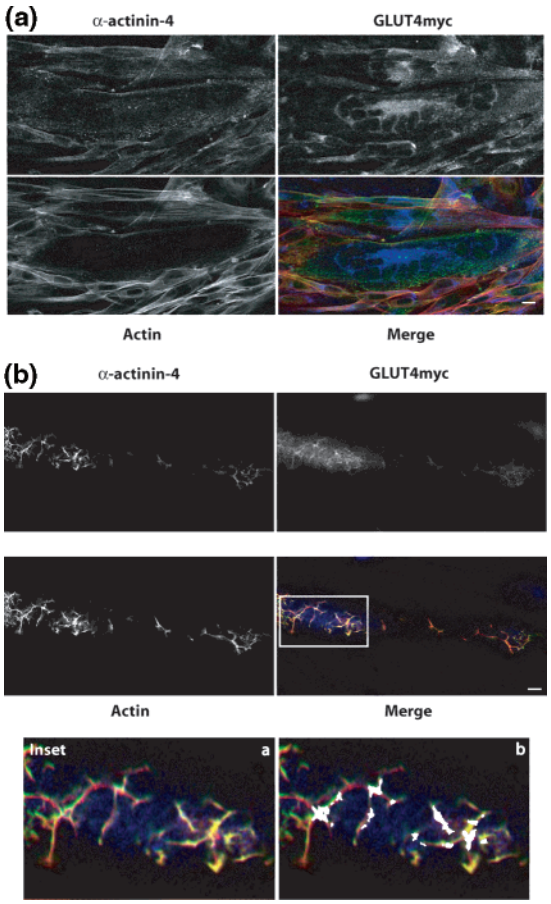

Figure 6. Insulin-dependent association of GLUT4*myc* with α-actinin-4 detected by immunofluorescence microscopy. L6-GLUT4*myc* myotubes grown on glass coverslips were serum-deprived for 4.5 h and subsequently treated **(a)** without or **(b)** with 100 nM insulin for 5 min at 37 °C. α-Actinin-4, GLUT4*myc* and actin were detected using a rabbit polyclonal anti-α-actinin-4 IgG/ anti-rabbit Alexa 488-IgG conjugate (green); mouse monoclonal anti-*myc* epitope (9E10) IgG/ anti-mouse Cy5-IgG conjugate (blue); and rhodamine-phalloidin (red), respectively, as described in Experimental Procedures. The processed samples were examined with a Zeiss LSM 510 laser scanning confocal microscope. The scale bar represents 10 μm. Shown is the fluorescence images of a L6-GLUT4myc myotube at **(a)** ≈ 2 μm above the coverslip and **(b)** ≈ 4 μm above the coverslip for each individual protein (shown in gray scale) and a deconvolved three-color merge. In **(b)** a close-up of the outlined region of the Merge is shown in Insets a and b. Distinct regions of coincidence are white in the three-color 'Merge' (Inset a). The regions of coincidence (volumes) for all three proteins within the deconvolved confocal plane shown in Inset a was calculated using Volocity 3.0 software (Improvision) as described in Experimental Procedures and illustrated as white overlays in Inset b.

derived peptide,[9] L-3-hydroxyacyl-CoA dehydrogenase;[10] and mUbc9[12,39] as putative GLUT4 ligands. On the other hand, glutathione-s-transferase-fusion proteins of the C-terminus of GLUT4 used to identify GLUT4 interacting proteins from cytosolic extracts of 3T3-L1 or isolated rat adipocytes, yielded GTB70 and aldolase as possible GLUT4-partners.[8,11] Other ligand proteins include Daxx and TUG and a couple of unidentified polypeptides, as reviewed recently.[13] Immunoprecipitation of full-length *native* GLUT4 has not been used to date to identify binding proteins, possibly because the main antigenic region of GLUT4 is its cytosol-facing C-terminus. Hence, binding of the immunoprecipitating antibody and ligand proteins might be mutually exclusive.

To circumvent these potential confounding factors, and to detect insulin-dependent interactive partners of GLUT4, we have immunoprecipitated stably expressed GLUT4*myc* from muscle cells via the *myc* epitope. The location of the epitope between transmembrane domains 1 and 2 of GLUT4 is unlikely to face the cytosol at any stage of the cycling of the protein, and hence should not interfere with the binding of endogenous intracellular proteins with the transporter. Second and most importantly, we implemented the SILAC approach to identify proteins that bind GLUT4 in an insulin-regulated fashion.

Proteins that Associate Differentially with GLUT4 in Response to Insulin. The principle of SILAC is that proteins that interact with the target (GLUT4*myc*) in a differential manner in two conditions (e.g., basal and insulin-stimulated cells) can be differentiated if the cultures exposed to these two conditions

were differentially labeled metabolically (with LeuD0 or LeuD3, respectively) prior to experimental manipulation. By this approach, contaminating proteins sedimenting with the immunoprecipitates, or proteins interacting with GLUT4 in a tonic non insulin-regulated manner, will show peptides of equal intensities in the LeuD3 and LeuD0 labeled state (insulin: control ratio of 1). Insulin:control ratios of individual proteins ≥ 1.5 or ≤ 0.66 repeatedly observed across all experiments were selected for further consideration. On the basis of these criteria, Table 1 lists the 36 identified proteins from 2 to 5 different experiments, which exhibit insulin-regulated association with GLUT4*myc*. By arranging these proteins into several functional categories, the table reveals some interesting trends: With the exception of sarcosin, all cytoskeletal proteins were elevated by insulin stimulation of the cells. This is in agreement with the requirement for cytoskeletal remodeling in GLUT4 translocation in response to insulin and in the localization of GLUT4 within a dynamic actin mesh in insulin-stimulated muscle cells.[40] Similarly, most traffic-related proteins, with the exception of NSF and the lysosomal Rab7 (which participates in all intracellular vesicle fusion events), were elevated by treatment with the hormone. Hence, the proteins listed in Table 1 may begin to identify unsuspected ligands that regulate GLUT4 localization and mobilization. Importantly, the hormone also elevated the interaction of GLUT4 with the glycolytic enzyme GAPDH, suggesting that a physical 'metabolon' may exist linking the glucose-procuring GLUT4 to the energy generating GAPDH/3-phosphoglycerate kinase complex. Notably, GAPDH can catalyze insulin-containing granule fusion with the membrane coupled to glycolytic flux,[41] and associates with cytoskeletal elements including microtubules.[42]

Another revelation from Table 1 is that insulin increases binding to GLUT4 of proteins involved in protein stabilization. Thus, with the exception of HSP86, interaction of protein-synthesis/folding related proteins with GLUT4 was potentiated by insulin stimulation. Conversely, insulin-treatment resulted in reduced association of GLUT4 with proteins involved in protein degradation via the proteasomal/ ubiquitination pathway.

The grouping of the type of proteins and their diversity underscores the discerning ability of the SILAC procedure applied to hormone action and further highlight the value of SILAC to identify dynamic interactions between proteins. Mapping their Gene Ontologies versus the Ontologies of all proteins identified here provides additional evidence of the significance of these 36 proteins. A higher fraction of the putative insulin-regulated GLUT4 binding partners (Table 1) belonged to the GO categories of generation of precursor metabolites and energy and monosaccharide metabolism, as would be expected from the known physiological roles of insulin related to the mobilization of this insulin regulated glucose transporter.

Proteins Regulating Protein Translation, Stability and Degradation. The gain in proteins involved in polypeptide stabilization observed in GLUT4*myc* immunoprecipitates along with the loss in proteins involved in polypeptide degradation is intriguing and suggests that insulin may acutely modulate the fate of GLUT4 by increasing its stabilization. Such a scenario would fit with the observations by Kandror et al. that the acquisition of insulin sensitivity during 3T3-L1 adipocyte differentiation is associated with improved stability of GLUT4[43,44] and by Giorgino et al. who speculated that binding of the sentrin-conjugating enzyme Ubc9 to GLUT4 prevents routing of the transporter to the protein degradation pathway.[12] In contrast, prolonged exposure of cultures to insulin, which causes insulin resistance, is associated with reduced GLUT4 half-life[45] or and retention in monosomes.[46] The results of the present study could lead to a systematic analysis of the significance of the differential binding to GLUT4 of proteins that regulate protein stability.

Proteins Involved in Vesicular Traffic Associated with GLUT4. Among vesicular-traffic related proteins found to increase in GLUT4 immunoprecipitates from insulin-stimulated cells Arfs 3 and 5 stand out, with Arf 4 displaying a ratio only slightly below 1.5 (see Supporting Table 1). The Arfs are small GTP binding proteins with several proposed functions in vesicle traffic and organellar integrity.[47] They may participate in GLUT4 budding from intracellular compartments upon insulin stimulation,[48] and association with GLUT4 may be reflective of the budding process elicited by the hormone. Future work should explore whether these Arfs interact directly with GLUT4 or through intermediates involved in vesicle generation, and should examine the subcellular locus of this interaction.

Recently, a protein named TUG was found to coprecipitate with $(myc)_7$GLUT4 expressed in 3T3-L1 adipocytes,[49] and we have reproduced this finding in immunoprecipitates of GLUT4-*myc* from L6 myoblasts and myotubes.[50] Preservation of the TUG-GLUT4*myc* interaction has an absolute requirement for alkylating agents presumably to stabilize the complex. However, such agents were not used for the immunoprecipitates analyzed herein by SILAC, and hence it is not surprising that TUG did not show up in the list of GLUT4 binding proteins (Table 1 and Supplementary Table 1).

Cytoskeletal Proteins Associated with GLUT4. The increased presence of cytoskeletal proteins in GLUT4*myc* immunoprecipitates from insulin-stimulated cells is compelling, given the ample evidence of cytoskeletal participation in GLUT4 translocation to the plasma membrane in response to insulin.[37,51−56] The increased presence of cofilin in GLUT4 immunoprecipitates from insulin-stimulated cells raises the possibility that the transporter directly interacts with proteins coordinating actin remodeling, or alternatively, forms multi-protein complexes with them. That cofilin may be a sensor of insulin signals is suggested from our observation that this actin-severing protein is dephosphorylated (and hence activated) in response to insulin (Patel, N. and Klip, A., unpublished observations). Among the cytoskeletal proteins that were increased >1.3 and <1.5 with insulin stimulation, γ-filamin (filamin C) emerges as an attractive GLUT4 ligand. γ-Filamin is also an actin-binding protein thought to stabilize three-dimensional networks of actin filaments and to link them to cell membranes. It is abundant in skeletal muscle where it was very recently shown to be phosphorylated in response to insulin and to be an Akt substrate.[57]

Most notable among cytoskeletal proteins found to sediment with GLUT4 in an insulin-dependent fashion was α-actinin-4. Importantly, this protein was also detected in a two-hybrid screen of a 3T3-L1 adipocyte library performed using as bait a hybrid protein encoding all the major cytosolic regions of GLUT4 in tandem (T. A. Gustafson and L. M. Kozma, personal communication and confirmed by us, X. Huang, P. J. Bilan and A. Klip, unpublished). Hence, it is possible that α-actinin-4 and GLUT4 interact directly rather than through an intermediate protein. Strikingly, the subcellular distribution and activity (actin bundling) of α-actinin proteins are affected by the interaction with phosphatidylinositol 3-kinase and its product

PI 3,4,5-P_3.[58−60] Hence, it is tempting to speculate that insulin may regulate the binding of α-actinin-4 to GLUT4 via input from the phosphatidylinositol 3-kinase pathway. Indeed, this pathway is essential for GLUT4 mobilization to the cell surface.

In contrast to its other three isoforms, α-actinin-4 is not part of adherent plaques or Z disks. Instead, α-actinin-4 is an actin-bundling protein (through its N-terminal domain), involved in generating loosely packed actin bundles. Such a loose F-actin structure allows myosins to interact within the actin bundle, resulting in a contractile structure. The formation of this unique, stimulus-induced structure raises the intriguing possibility that α-actinin-4 links GLUT4 (likely through its spectrin repeat regions) to actin filaments in the course of the translocation of the transporter to the membrane. Here, we further confirm that α-actinin-4 coprecipitates with GLUT4*myc* in an insulin-dependent fashion, by immunoblotting GLUT4*myc* immunoprecipitates with isoform-specific antibodies to α-actinin-4. No such coprecipitation of α-actinin-4 was observed in immunoprecipitation experiments that used wild-type L6 muscle cells (i.e., cells without GLUT4*myc*). The interaction of GLUT4 with α-actinin-4 may occur in the context of a viable actin cytoskeleton, since interfering with actin filament dynamics via latrunculin B reduced markedly the interaction between GLUT4*myc* and α-actinin-4. Such a scenario was further substantiated by immunofluorescence, showing discernible co-localization of GLUT4*myc* with α-actinin-4 in response to insulin-stimulation and this occurred in areas of active actin remodeling. Notably, no colocalization was observed between GLUT4myc and α-actinin-4 or α-actinin-4 and actin in unstimulated cells (basal state) where GLUT4*myc* showed its characteristic perinuclear localization[38] and filamentous actin mainly forms stress fibers. In insulin-stimulated myotubes a subset of GLUT4 molecules relocate to zones of remodeled actin where there was significant colocalization of α-actinin-4, GLUT4*myc* and actin in dorsal projections of the membrane (Figure 6). The remaining perinuclear GLUT4 still failed to colocalize with the cytoskeletal proteins. The observations that α-actinin-4 and GLUT4*myc* colocalize in an insulin-dependent manner within dorsal-membrane actin-rich structures buttress the hypothesis that α-actinin-4 has a role in GLUT4 vesicle arrival at the plasma membrane.[4] The findings of this work constitute a stepping-stone for an in-depth analysis of the role of α-actinin-4 in GLUT4 traffic, and open the door to study the role of other proteins listed in Table 1.

Abbreviations: GLUT4, GLUcose Transporter, isoform 4; HRP, Horse-Radish Peroxidase; SILAC, Stable Isotope Labelling by Amino acids in Cell culture; STAGE, STop And Go Extraction; TM, Total Membranes; GO, Gene Ontology.

Acknowledgment. We thank Dr. Shao-En Ong and Peter Mortensen for programmatic assistance and members of CEBI for fruitful discussions. We thank Drs. Thomas A. Gustafson and Lynn M. Kozma of Metabolex, Inc. Hayward, CA (LMK is currently with Cepheid, Sunnyvale, CA) for sharing the yeast-two-hybrid α-actinin-4 clone that interacts with GLUT4. This work was supported by grants from the Canadian Institutes of Health Research (CIHR MT12601) and the Canadian Diabetes Association to A.K., and a grant from the Danish National Research Foundation to CEBI to M.M.. L.J.F. was supported by a postdoctoral long-term fellowship from the European Molecular Biology Organization (EMBO). A.R. and M.F. were supported by postdoctoral fellowships from the Research Training Centre at The Hospital for Sick Children. N.P. was supported by a studentship from the CIHR. X.H. was supported by a by postdoctoral fellowship from the Banting and Best Diabetes Centre, University of Toronto. The LTQ-FT is a kind loan from the Max Planck Institute for Biochemistry, Martinsried, Germany.

Supporting Information Available: Supporting Table 1. GLUT4*myc*-associating proteins. Listed are all the proteins identified in this study that associated with the GLUT4*myc* anti-*myc* immunoprecipitation. IPI and UniProt accession numbers for each protein are given, along with the protein name and the measured insulin:control ratio ± standard error of the mean (SEM). In addition, the number of peptides used for quantification, the sequence coverage achieved for each protein, the total number of amino acids in each protein sequence, the total number of peptides identified for each protein and the amino acid sequence of each peptide are also listed. This material is available free of charge via the Internet at http://pubs.acs.org.

References

(1) Joost, H. G.; Bell, G. I.; Best, J. D.; Birnbaum, M. J.; Charron, M. J.; Chen, Y. T.; Doege, H.; James, D. E.; Lodish, H. F.; Moley, K. H.; Moley, J. F.; Mueckler, M.; Rogers, S.; Schurmann, A.; Seino, S.; Thorens, B. Nomenclature of the GLUT/SLC2A family of sugar/polyol transport facilitators. *Am. J. Physiol. Endocrinol. Metab.* **2002**, *282*, E974−976.

(2) Rudich, A.; Konrad, D.; Torok, D.; Ben-Romano, R.; Huang, C.; Niu, W.; Garg, R. R.; Wijesekara, N.; Germinario, R. J.; Bilan, P. J.; Klip, A. Indinavir uncovers different contributions of GLUT4 and GLUT1 towards glucose uptake in muscle and fat cells and tissues. *Diabetologia 46*, **2003**, 649−658.

(3) Bryant, N. J.; Govers, R.; James, D. E. Regulated transport of the glucose transporter GLUT4. *Nat. Rev. Mol. Cell. Biol.* **2002**, *3*, 267−277.

(4) Rudich, A.; Klip, A. Push/pull mechanisms of GLUT4 traffic in muscle cells. *Acta Physiol. Scand.* **2003**, *178*, 297−308.

(5) Watson, R. T.; Kanzaki, M.; Pessin, J. E. Regulated membrane trafficking of the insulin-responsive glucose transporter 4 in adipocytes. *Endocr. Rev.* **2004**, *25*, 177−204.

(6) Gaster, M.; Staehr, P.; Beck-Nielsen, H.; Schroder, H. D.; Handberg, A. GLUT4 is reduced in slow muscle fibers of type 2 diabetic patients: is insulin resistance in type 2 diabetes a slow, type 1 fiber disease? *Diabetes* **2001**, *50*, 1324−1329.

(7) Shi, Y.; Liu, H.; Vanderburg, G.; Samuel, S. J.; Ismail-Beigi, F.; Jung, C. Y. Modulation of GLUT1 intrinsic activity in clone 9 cells by inhibition of oxidative phosphorylation. *J. Biol. Chem.* **1995**, *270*, 21772−21778.

(8) Liu, H.; Xiong, S.; Shi, Y.; Samuel, S. J.; Lachaal, M.; Jung, C. Y. ATP-sensitive binding of a 70-kDa cytosolic protein to the glucose transporter in rat adipocytes. *J. Biol. Chem.* **1995**, *270*, 7869−7875.

(9) Lee, W.; Samuel, J.; Zhang, W.; Rampal, A. L.; Lachaal, M.; Jung, C. Y. A myosin-derived peptide C109 binds to GLUT4-vesicles and inhibits the insulin-induced glucose transport stimulation and GLUT4 recruitment in rat adipocytes. *Biochem. Biophys. Res. Commun.* **1997**, *240*, 409−414.

(10) Shi, Y.; Samuel, S. J.; Lee, W.; Yu, C.; Zhang, W.; Lachaal, M.; Jung, C. Y. Cloning of an L-3-hydroxyacyl-CoA dehydrogenase that interacts with the GLUT4 C-terminus. *Arch. Biochem. Biophys.* **1999**, *363*, 323−332.

(11) Kao, A. W.; Noda, Y.; Johnson, J. H.; Pessin, J. E.; Saltiel, A. R. Aldolase mediates the association of F-actin with the insulin-responsive glucose transporter GLUT4. *J. Biol. Chem.* **1999**, *274*, 17742−17747.

(12) Giorgino, F.; de Robertis, O.; Laviola, L.; Montrone, C.; Perrini, S.; McCowen, K. C.; Smith, R. J. The sentrin-conjugating enzyme mUbc9 interacts with GLUT4 and GLUT1 glucose transporters and regulates transporter levels in skeletal muscle cells. *Proc. Natl. Acad. Sci. U.S.A.* **2000**, *A 97*, 1125−1130.

(13) Ishiki, M.; Klip, A. 2005 Recent Developments in the Regulation of Glucose Transporter-4 Traffic: New Signals, Locations and Partners. *Endocrinology*, Epub ahead of print.

(14) Ho, Y.; Gruhler, A.; Heilbut, A.; Bader, G. D.; Moore, L.; Adams, S. L.; Millar, A.; Taylor, P.; Bennett, K.; Boutilier, K.; Yang, L.; Wolting, C.; Donaldson, I.; Schandorff, S.; Shewnarane, J.; Vo, M.; Taggart, J.; Goudreault, M.; Muskat, B.; Alfarano, C.; Dewar, D.;

Lin, Z.; Michalickova, K.; Willems, A. R.; Sassi, H.; Nielsen, P. A.; Rasmussen, K. J.; Andersen, J. R.; Johansen, L. E.; Hansen, L. H.; Jespersen H.; Podtelejnikov, A.; Nielsen, E.; Crawford, J.; Poulsen, V.; Sorensen, B. D.; Matthiesen, J.; Hendrickson, R. C.; Gleeson, F.; Pawson, T.; Moran, M. F.; Durocher, D.; Mann, M.; Hogue, C. W.; Figeys, D.; Tyers, M. Systematic identification of protein complexes in *Saccharomyces cerevisiae* by mass spectrometry. *Nature* **2002**, *415*, 180−183.

(15) Gavin, A. C.; Bosche, M.; Krause, R.; Grandi, P.; Marzioch, M.; Bauer, A.; Schultz, J.; Rick, J. M.; Michon, A. M.; Cruciat, C. M.; Remor, M.; Hofert, C.; Schelder, M.; Brajenovic, M.; Ruffner, H.; Merino, A.; Klein, K.; Hudak, M.; Dickson, D.; Rudi, T.; Gnau, V.; Bauch, A.; Bastuck, S.; Huhse, B.; Leutwein, C.; Heurtier, M. A.; Copley, R. R.; Edelmann, A.; Querfurth, E.; Rybin, V.; Drewes, G.; Raida, M.; Bouwmeester, T.; Bork, P.; Seraphin, B.; Kuster, B.; Neubauer, G.; Superti-Furga, G. Functional organization of the yeast proteome by systematic analysis of protein complexes. *Nature* **2002**, *415*, 141−147.

(16) Washburn, M. P.; Wolters, D.; Yates, J. R., 3rd. Large-scale analysis of the yeast proteome by multidimensional protein identification technology. *Nat. Biotechnol.* **2001**, *19*, 242−247.

(17) Steen, H.; Mann, M. The ABC's (and XYZ's) of peptide sequencing. *Nat. Rev. Mol. Cell. Biol.* **2004**, *5*, 699−711.

(18) Olsen, J. V.; Ong, S. E.; Mann, M. Trypsin cleaves exclusively C-terminal to arginine and lysine residues. *Mol. Cell. Proteomics* **2004**, *3*, 608−614.

(19) Ong, S. E.; Blagoev, B.; Kratchmarova, I.; Kristensen, D. B.; Steen, H.; Pandey, A.; Mann, M. Stable isotope labeling by amino acids in cell culture, SILAC, as a simple and accurate approach to expression proteomics. *Mol. Cell. Proteomics* **2002**, *1*, 376−386.

(20) de Hoog, C. L.; Foster, L. J.; Mann, M. RNA and RNA binding proteins participate in early stages of cell spreading through spreading initiation centers. *Cell* **2004**, *117*, 649−662.

(21) Blagoev, B.; Kratchmarova, I.; Ong, S. E.; Nielsen, M.; Foster, L. J.; Mann, M. A proteomics strategy to elucidate functional protein−protein interactions applied to EGF signaling. *Nat. Biotechnol.* **2002**, *21*, 315−318.

(22) Schulze W. X.; Mann M. A novel proteomic screen for peptide−protein interactions. *J. Biol. Chem.* **2004**, *279*, 10756−10764.

(23) Ranish, J. A.; Yi, E. C.; Leslie, D. M.; Purvine, S. O.; Goodlett, D. R.; Eng, J.; Aebersold, R. The study of macromolecular complexes by quantitative proteomics. *Nat. Genet.* **2003**, *33*, 349−355.

(24) Gygi, S. P.; Rist, B.; Gerber, S. A.; Turecek, F.; Gelb, M. H.; Aebersold, R. Quantitative analysis of complex protein mixtures using isotope-coded affinity tags. *Nat. Biotechnol.* **1999**, *17*, 994−999.

(25) Mitsumoto, Y.; Burdett, E.; Grant, A.; Klip, A. Differential expression of the GLUT1 and GLUT4 glucose transporters during differentiation of L6 muscle cells. *Biochem. Biophys. Res. Commun.* **1991**, *175*, 652−659.

(26) Foster, L. J.; de Hoog, C. L.; Mann, M. Unbiased quantitative proteomics of lipid rafts reveals high specificity for signaling factors. *Proc. Natl. Acad. Sci., U.S.A.* **2003**, *100*, 5813−5818.

(27) Wilm, M.; Shevchenko, A.; Houthaeve, T.; Breit, S.; Schweigerer, L.; Fotsis, T.; Mann, M. Femtomole sequencing of proteins from polyacrylamide gels by nano-electrospray mass spectrometry. *Nature* **1996**, *379*, 466−469.

(28) Rappsilber, J.; Ishihama, Y.; Mann, M. Stage(STop And Go Extraction) tips for MALDO, nanoelectrospray, and LC/MS sample pretreatment in proteomics. *Anal. Chem.* **2003**, *175*, 663−670.

(29) Rappsilber, J.; Ryder, U.; Lamond, A. I.; Mann, M. Large-scale proteomic analysis of the human spliceosome. *Genome Res.* **2002**,*12*, 1231−1245.

(30) Zeeberg, B. R.; Feng, W.; Wang, G.; Wang, M. D.; Fojo, A. T.; Sunshine, M.; Narasimhan, S.; Kane, D. W.; Reinhold, W. C.; Lababidi, S.; Bussey, K. J.; Riss, J.; Barrett, J. C.; Weinstein, J. N. GoMiner: a resource for biological interpretation of genomic and proteomic data. *Genome Biol.* **2003**, *4*, R28.

(31) Khayat, Z. A.; Tong, P.; Yaworsky, K.; Bloch, R. J.; Klip, A. Insulin-induced actin filament remodeling colocalizes actin with phosphatidylinositol 3-kinase and GLUT4 in L6 myotubes. *J. Cell. Sci.* **2000**, *113* Pt 2, 279−290.

(32) Aebersold, R.; Mann, M. Mass spectrometry-based proteomics. *Nature* **2003**, *422*, 198−207.

(33) Ong, S. E.; Blagoev, B.; Kratchmarova, I.; Kristensen, D. B.; Steen, H.; Pandey, A.; Mann, M. Stable Isotope Labeling by Amino Acids in Cell Culture, SILAC, as a Simple and Accurate Approach to Expression Proteomics. *Mol. Cell. Proteomics* **2002**, *1*, 376−386.

(34) Ashburner, M.; Ball, C. A.; Blake, J. A.; Botstein, D.; Butler, H.; Cherry, J. M.; Davis, A. P.; Dolinski, K.; Dwight, S. S.; Eppig, J. T.; Harris, M. A.; Hill, D. P.; Issel-Tarver, L.; Kasarskis, A.; Lewis, S.; Matese, J. C.; Richardson, J. E.; Ringwald, M.; Rubin, G. M.; Sherlock, G. Gene ontology: tool for the unification of biology. The Gene Ontology Consortium. *Nat. Genet.* **2000**, *25*, 25−29.

(35) Ikemoto, A.; Bole, D. G.; Ueda, T. Glycolysis and glutamate accumulation into synaptic vesicles. Role of glyceraldehyde phosphate dehydrogenase and 3-phosphoglycerate kinase. *J. Biol. Chem.* **2003**, *278*, 5929−5940.

(36) Torok, D.; Patel, N.; Jebailey, L.; Thong, F. S.; Randhawa, V. K.; Klip, A.; Rudich, A. Insulin but not PDGF relies on actin remodeling and on VAMP2 for GLUT4 translocation in myoblasts. *J. Cell. Sci.* **2004**, *117*, 5447−5455.

(37) Tong, P.; Khayat, Z. A.; Huang, C.; Patel, N.; Ueyama, A.; Klip, A. Insulin-induced cortical actin remodeling promotes GLUT4 insertion at muscle cell membrane ruffles. *J. Clin. Invest.* **2001**, *108*, 371−381.

(38) Patel, N.; Rudich, A.; Khayat, Z. A.; Garg, R.; Klip, A. Intracellular segregation of phosphatidylinositol-3,4,5-trisphosphate by insulin-dependent actin remodeling in L6 skeletal muscle cells. *Mol. Cell. Biol.* **2003**, *23*, 4611−4626.

(39) Lalioti, V. S.; Vergarajauregui, S.; Pulido, D.; Sandoval, I. V. The insulin-sensitive glucose transporter, GLUT4, interacts physically with Daxx. Two proteins with capacity to bind Ubc9 and conjugated to SUMO1. *J. Biol. Chem.* **2002**, *277*, 19783−19791.

(40) Patel, N.; Huang, C.; Klip, A. (2005) Cellular location of insulin-triggered signals and implications for glucose transport. *Pfluger's Archiv.*, in press.

(41) Han, X.; Ramanadham, S.; Turk, J.; Gross, R. W. Reconstitution of membrane fusion between pancreatic islet secretory granules and plasma membranes: catalysis by a protein constituent recognized by monoclonal antibodies directed against glyceraldehyde-3-phosphate dehydrogenase. *Biochim. Biophys. Acta* **1998**, *1414*, 95−107.

(42) Tisdale, E. J. Glyceraldehyde-3-phosphate dehydrogenase is phosphorylated by protein kinase Ciota /lambda and plays a role in microtubule dynamics in the early secretory pathway. *J. Biol. Chem.* **2002**, *277*, 3334−3341.

(43) El-Jack, A. K.; Kandror, K. V.; Pilch, P. F. The formation of an insulin-responsive vesicular cargo compartment is an early event in 3T3-L1 adipocyte differentiation. *Mol. Biol. Cell.* **1999**, *10*, 1581−1594.

(44) Shi, J.; Kandror, K. V. Sortilin is essential and sufficient for the formation of Glut4 storage vesicles in 3T3-L1 adipocytes. *Dev. Cell.* **2005**, *9*, 99−108.

(45) Sargeant, R. J.; Paquet, M. R. Effect of insulin on the rates of synthesis and degradation of GLUT1 and GLUT4 glucose transporters in 3T3-L1 adipocytes. *Biochem. J.* **1993**, *290* (Pt 3), 913−919.

(46) Taha, C.; Liu, Z.; Jin, J.; Al-Hasani, H.; Sonenberg, N.; Klip, A. Opposite translational control of GLUT1 and GLUT4 glucose transporter mRNAs in response to insulin. Role of mammalian target of rapamycin, protein kinase b, and phosphatidylinositol 3-kinase in GLUT1 mRNA translation. *J. Biol. Chem.* **1999**, *274*, 33085−33091.

(47) Nie, Z.; Hirsch, D. S.; Randazzo, P. A. Arf and its many interactors. *Curr. Opin. Cell. Biol.* **2003**, *15*, 396−404.

(48) Millar, C. A.; Powell, K. A.; Hickson, G. R.; Bader, M. F.; Gould, G. W. Evidence for a role for ADP-ribosylation factor 6 in insulin-stimulated glucose transporter-4 (GLUT4) trafficking in 3T3-L1 adipocytes. *J. Biol. Chem.* **1999**, *274*, 17619−17625.

(49) Bogan, J. S.; Hendon, N.; McKee, A. E.; Tsao, T. S.; Lodish, H. F. Functional cloning of TUG as a regulator of GLUT4 glucose transporter trafficking. *Nature* **2003**, *425*, 727−733.

(50) Huang, X.; Rudich, A.; Wijesekara, N.; Bilan, P. J.; Klip, A. The protein TUG is associated with GLUT4 in L6 muscle cells. *Keystone Symposium on Diabetes Mellitus: Molecular Signaling, Genes and Therapeutics*; Banff, Alberta, March 4−10. 2004.

(51) Tsakiridis, T.; Vranic, M.; Klip, A. Disassembly of the actin network inhibits insulin-dependent stimulation of glucose transport and prevents recruitment of glucose transporters to the plasma membrane. *J. Biol. Chem.* **1994**, *269*, 29934−29942.

(52) Wang, Q.; Bilan, P. J.; Tsakiridis, T.; Hinek, A.; Klip, A. Actin filaments participate in the relocalization of phosphatidylinositol3-kinase to glucose transporter-containing compartments and in the stimulation of glucose uptake in 3T3-L1 adipocytes. *Biochem. J.* **1998**, *331* (Pt 3), 917−928.

(53) Patki, V.; Buxton, J.; Chawla, A.; Lifshitz, L.; Fogarty, K.; Carrington, W.; Tuft, R.; Corvera, S. Insulin action on GLUT4 traffic visualized in single 3T3-l1 adipocytes by using ultrafast microscopy. *Mol. Biol. Cell.* **2001**, *12*, 129−141.
(54) Kanzaki, M.; Pessin, J. E. Insulin-stimulated GLUT4 translocation in adipocytes is dependent upon cortical actin remodeling. *J. Biol. Chem.* **2001**, *276*, 42436−42444.
(55) Kanzaki, M.; Watson, R. T.; Khan, A. H.; Pessin, J. E. Insulin stimulates actin comet tails on intracellular GLUT4-containing compartments in differentiated 3T3L1 adipocytes. *J. Biol. Chem.* **2001**, *276*, 49331−49336.
(56) Jiang, Z. Y.; Chawla, A.; Bose, A.; Way, M.; Czech, M. P. A phosphatidylinositol 3-kinase-independent insulin signaling pathway to N−WASP/Arp2/3/F-actin required for GLUT4 glucose transporter recycling. *J. Biol. Chem.* **2002**, *277*, 509−515.
(57) Murray, J. T.; Campbell, D. G.; Peggie, M.; Alfonso, M.; Cohen, P. Identification of filamin C as a new physiological substrate of PKBalpha using KESTREL. *Biochem. J.* **2004**, *384*, 489−494.
(58) Greenwood, J. A.; Theibert, A. B.; Prestwich, G. D.; Murphy-Ullrich, J. E. Restructuring of focal adhesion plaques by PI 3-kinase. Regulation by PtdIns (3,4,5)-p(3) binding to alpha-actinin. *J. Cell. Biol.* **2000**, *150*, 627−642.
(59) Fraley, T. S.; Tran, T. C.; Corgan, A. M.; Nash, C. A.; Hao, J.; Critchley, D. R.; Greenwood, J. A. Phosphoinositide binding inhibits alpha-actinin bundling activity. *J. Biol. Chem.* **2003**, *278*, 24039−24045.
(60) Shibasaki, F.; Fukami, K.; Fukui, Y.; Takenawa, T. Phosphatidylinositol 3-kinase binds to alpha-actinin through the p85 subunit. *Biochem. J.* **1994**, *302* (Pt 2), 551−557.

PR0502626